Small-scale density fluctuation modes in a Hall plasma thruster: experimental studies via collective light scattering

IEPC-2009-143

Presented at the 31st International Electric Propulsion Conference,
University of Michigan, Ann Arbor, Michigan, USA
September 20–24, 2009

Sedina Tsikata*, Dominique Grésillon†, Cyrille Honoré‡, and Vitaliy Pisarev§
Ecole Polytechnique, Laboratoire de Physique des Plasmas, UMR 7648, Palaiseau 91128, France

Nicolas Lemoine¶
Institut Jean Lamour, Université Henri Poincaré, Nancy 54506, France

Anomalous electron transport near the exit of the Hall thruster, where wall and electron-neutral collisions are scarce, is believed to be due to plasma oscillations. Azimuthal oscillations of frequencies on the order of a few MHz and of length scales on the order of the electron Larmor radius, propagating across magnetic field lines, have been identified for the first time experimentally using collective light scattering. The dispersion relations, scaling laws, directionality and fluctuation intensity of this mode have been determined.

Nomenclature

$\vec{k}$, k	= observation wave vector, wave number
$\vec{B}$	= magnetic field
$\vec{E}$	= electric field
$S(k,\omega)$	= dynamic form factor at wave number k and frequency ω
$S(k)$	= static form factor at wave number k
V_D	= azimuthal drift velocity

*PhD student, sedina.tsikata@polytechnique.edu
†Professor Emeritus, dominique.gresillon@polytechnique.edu
‡Research Engineer, cyrille.honore@polytechnique.edu
§Visiting Scientist, vitaliy.pisarev@lptp.polytechnique.fr
¶Assistant Professor, nicolas.lemoine@lpmi.uhp-nancy.fr

I. Introduction

The Hall thruster uses a crossed electric and magnetic field configuration to ionize and accelerate ions. It is widely used on communications satellites, and more recently, on interplanetary missions such as Deep Space 1 (NASA) and SMART-1 (ESA). The development of higher-powered thrusters is hindered by limited understanding of certain thruster phenomena, such as anomalous electron transport. Such transport is believed to contribute to reduced thruster performance.

PIC simulations developed by Adam et. al.[1] have succeeded in demonstrating the presence of high frequency, millimeter-scale oscillations which are likely to be at the origin of the anomalous transport near the thruster exit. These simulations required no arbitrary parameters to account for electron mobility, and the presence of the azimuthal drift was determined to be sufficient to induce transport, without the need for the inclusion of additional factors such as gradients in the magnetic field.

Confirming the presence of these instabilities is impossible through the use of conventional probes and antennae, because of the short length scales involved. Collective light scattering, commonly used in the study of tokamak plasmas[2], has therefore been adopted in our work for the identification of oscillations in a thruster plasma. A high-performance collective light scattering bench, PRAXIS, has been designed and used to identify small-scale oscillations in the thruster[3].

The characteristics of the collective light scattering diagnostic are presented in Section II. Section III describes observations concerning the azimuthal mode. The main conclusions are presented in Section IV.

II. The collective light scattering diagnostic PRAXIS

A. General characteristics of the optical bench

The optical bench PRAXIS (**PR**opulsion **A**nalysis e**X**periments via **I**nfrared **S**cattering) has been designed in two stages. The first version, PRAXIS-I, was built in 2008 and was upgraded in 2009 to PRAXIS-II, a bench with a wider range of accessible wave numbers and scanning angles. The experimental results in this paper were achieved using PRAXIS-II. The bench is installed during experiments at the PIVOINE thruster test facility in Orléans. Experiments are performed on a PPS®-X000ML experimental Hall thruster, a high-powered, 5 kW model designed by Snecma. The thruster uses Xe as propellant.

PRAXIS uses a continuous, 40 W, CO_2, monomode laser of wavelength 10.6 μm for scattering. The initial beam is split into two components: an intense primary beam, and a second "reference" beam known as the local oscillator, whose power is a few hundred mW and which is shifted 40 MHz with respect to the initial beam. The local oscillator interacts with the plasma-scattered signal, producing an interference field from which the magnitude and phase of the plasma-scattered signal may be readily recovered[4]. The primary and local oscillator intersect in front of the thruster exit plane and define the scattering volume. The observation wave vector is obtained from the Bragg relation,

$$\vec{k} = \vec{k_s} - \vec{k_o} \tag{1}$$

where $\vec{k}_s$ is the wave vector of the scattered light and $\vec{k}_o$ the wave vector of the incident primary beam (Fig. 1). The complex amplitude of the scattered electric field is known to be proportional to the spatial Fourier transform, at wave vector $\vec{k}$, of the electron density $n(\vec{r})$.

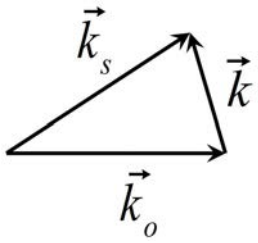

Figure 1. Definition of observation wave vector from scattered wave vector k_s and incident wave vector k_o

The beams waists in the measurement zone are set to 2.9 mm. The beams enter and exit the vacuum chamber through ZnSe windows on either side of the vessel. Upon exiting, they are recovered by a series of

mirrors. The primary beam is sent to an absorber, and the local oscillator and the plasma-scattered wave are sent to an HgCdTe detector on the bench. The time-varying detector current is demodulated to recover the amplitude and phase components of the scattered electric field, i.e. the spatial electron distribution at the selected $\vec{k}$ Fourier component.

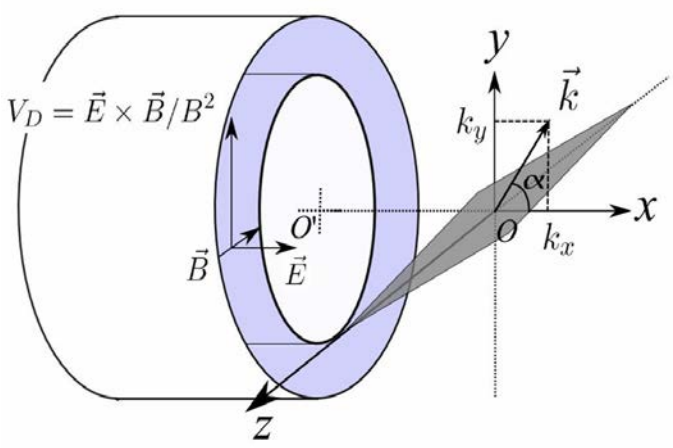

Figure 2. Scattering volume (dark gray) defined by the intersection of the primary and local oscillator beams. The inner plasma volume is in light gray. The coordinate system used has the radial magnetic field aligned with z, the axial electric field aligned with x, and the $\vec{E} \times \vec{B}$ drift velocity, V_D, aligned with y. Ox is coincident with the thruster axis.

B. Measurements

The measurement capabilities of the optical bench allow the variation of the angle α between $\vec{k}$ and Ox in the xOy plane (Fig. 2). α is measured from the x axis and increases in the anti-clockwise direction. The magnitude of k is varied between 4000 and 13200 rad/m, a range which is designed to cover an adequate wave number range at which the azimuthal instability is expected, namely, wavelengths on the order of the electron cyclotron radius.

The position of the measurement volume along y can be varied. When the measurement volume is on-axis (coincident with z), $\vec{k}$ is always perpendicular to $\vec{B}$, and the wave vector component parallel to $\vec{B}$, k_r, is at its smallest value (corresponding to the inverse of the channel width). The measurement volume can be translated in the direction of $+y$ or $-y$ to obtain different k_r components. At two extreme positions, where the measurement volume is placed at the top or bottom thruster channel, measurements with $\vec{k}$ aligned parallel to $\vec{B}$ may be made.

The characteristics of the fluctuations are obtained from analyses of the frequency spectra. These spectra are obtained from a combination of a Fourier analysis on several sequential time series and an averaging procedure. The spectra are then corrected in order to eliminate the contributions of the thermal and photonic noise. The normalized spectrum is the dynamic form factor $S(k, \omega)$, in units of s, which provides the intensity of the fluctuation at a particular wave number over a range of frequencies. Figure 3 shows an example of a normalized spectrum obtained when k is aligned parallel to $\vec{E} \times \vec{B}$. For this mode, in the wave number range used, frequency peaks are typically observed between 1 and 10 MHz. The frequency peak is integrated over an appropriate range to yield the static form factor $S(k)$,

$$S(k) = \int S(k, \omega) \frac{d\omega}{2\pi} \tag{2}$$

which is a measure of the absolute magnitude of the fluctuation at a particular wave number. $S(k)$ is a dimensionless quantity.

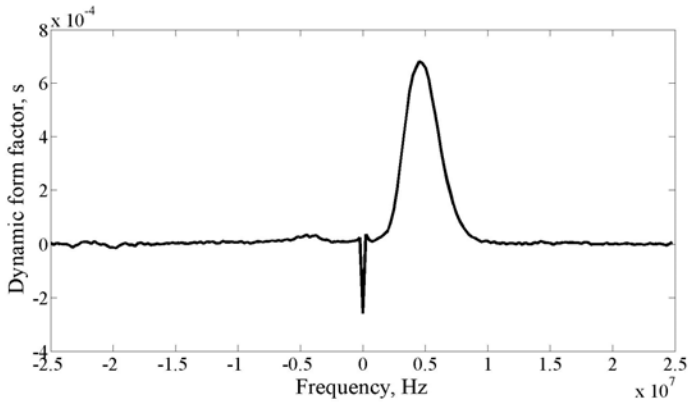

Figure 3. Normalized frequency spectrum. In this example, $\vec{k}$ is aligned parallel to $\vec{E} \times \vec{B}$ and has a magnitude of 9630 rad/m. A large signal peak is evident near 5 MHz.

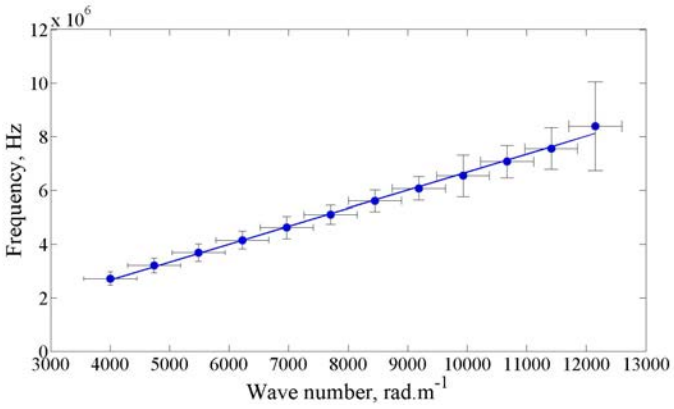

Figure 4. Characteristic dispersion relation of $\vec{E} \times \vec{B}$ mode.

III. Characteristics of the $\vec{E} \times \vec{B}$ mode

A. Dispersion relation

Henceforth, the mode observed when $\vec{k}$ is oriented parallel, or nearly parallel to, the $\vec{E} \times \vec{B}$ drift direction is known as the $\vec{E} \times \vec{B}$ mode. Unless otherwise stated, the thruster is operated at 18 mg/s in all experiments, with a discharge voltage of 300 V, and the thruster is located an axial distance of 17 mm from the measurement volume center, with the measurement volume aligned with O'. A typical variation of the peak frequency as a function of k_y is shown in Fig. 4. In this experiment, the optical alignment was changed to vary the modulus of $\vec{k}$, while maintaining the orientation of $\vec{k}$ along k_y.

The dispersion relation is linear and continuous, and a velocity of 4.21×10^3 m/s is obtained from the slope. Although an ion acoustic mode is not expected to propagate across $\vec{B}$, it is interesting to observe that the velocity is of the same order of magnitude as that of an ion acoustic mode propagating in a Xe plasma of electron temperature 24 eV. The dispersion relation obtained from purely 2D linear theory (for a wave propagating in the plane xOy) is discrete and the instability is predicted to occur at certain wave number values only (those which allow for a resonance condition to be satisfied). However, very recent work by A. Héron on the 3D dispersion relation demonstrates that the presence of a small k_r component is sufficient to render the dispersion relation continuous.

The frequencies and wave numbers for the wave predicted in theory are close to those obtained experimentally, provided a sufficient k_r component is included in the theory.

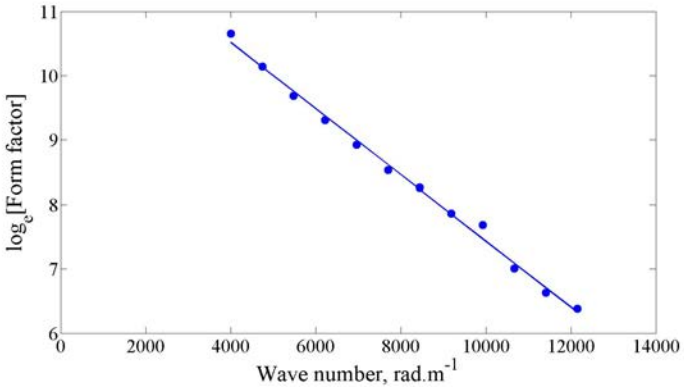

Figure 5. $\log_e$ (Form factor) variation with k for $\vec{E} \times \vec{B}$ mode.

B. Form factor scaling with length scale

The natural logarithm of the form factor is plotted against wave number in Fig. 5. This example corresponds to the form factors determined at each wave number in Fig. 4. The form factor has an exponential dependence on k,

$$S(k) = S_0 e^{-bk} \tag{3}$$

The total density fluctuation is obtained from an integration of $S(k)$ over the entire k-space, and Eq. 3 will be used for this purpose. Eq. 3 is used to determine the parameters for another experiment (in which the maximum form factors were obtained, on the order of 10^5. The corresponding extrapolated value for the maximum intensity measured is $S_0 = 4.6{\times}10^6$, while the characteristic decrement length, b, is $6.78{\times}10^{-4}$ m.

C. Spatial distribution in the (k_x, k_y) plane

A determination of the directionality of mode in the xOy plane provides clues as to how it propagates and is used to determine the density fluctuation rate. Such a determination is performed by varying α around $90°$.

Figure 6 shows the form factor variation with α. The maximum amplitude of the mode occurs not when k is aligned parallel to $\vec{E} \times \vec{B}$, but at an inclination of $10.6°$ towards the thruster (a mean value determined from a number of experiments). This is an indication that the classic view of the azimuthal mode propagating purely parallel to $\vec{E} \times \vec{B}$ must be revised.

The angular extension in the xOy plane of this mode is obtained from a determination of the Gaussian peak width, from which the peak-broadening effect of the device resolution has been removed. The result is an α extension, σ_α, of only $3.6°$, an indication that this mode propagates within a restricted region.

Two additional cases have been investigated, with the measurement volume situated at the top and bottom thruster channels. For these cases, an exploration around $90°$ reveals no signal; this is expected because at these positions, $\vec{k}$ is oriented parallel and anti-parallel to $\vec{B}$ (and orthogonal to $\vec{E} \times \vec{B}$). Density fluctuations parallel to $\vec{B}$ are negligible compared to those perpendicular to $\vec{B}$.

D. Spatial distribution in the (k_y, k_z) plane

The characterization of the mode is completed with a determination of its direction in the yOz plane. This experiment requires that the measurement volume be translated along y and a measurement of the mode intensity performed at different heights h, illustrated in Fig. 7. Each height corresponds to different magnitudes of the k_r component. In Fig. 7, polar coordinates are used to reflect the fact that the k_r component is parallel to the radial $\vec{B}$ field at every point on the thruster azimuth, while k_β is always parallel to V_D.

The angle β (Fig. 7) is obtained from the ratio h/R, where R is the mean thruster radius of 62.5 mm (the distance from O' to the center of the channel). As the height is changed, the wave number is kept constant,

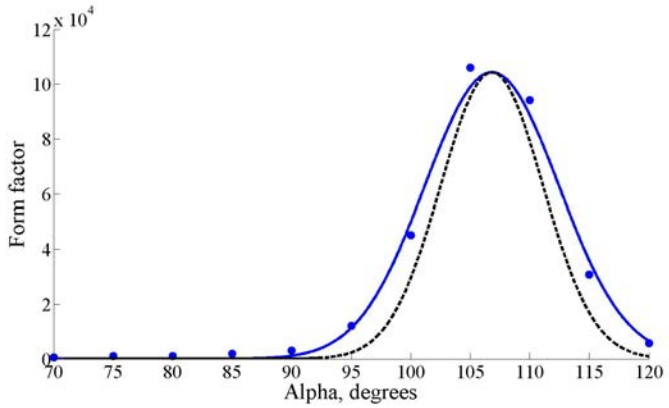

Figure 6. Form factor of $\vec{E} \times \vec{B}$ mode with α. The experimentally-determined points are in blue, and the Gaussian fit shown in the blue full line. The natural width due to the resolution of the device is indicated by the black dotted line.

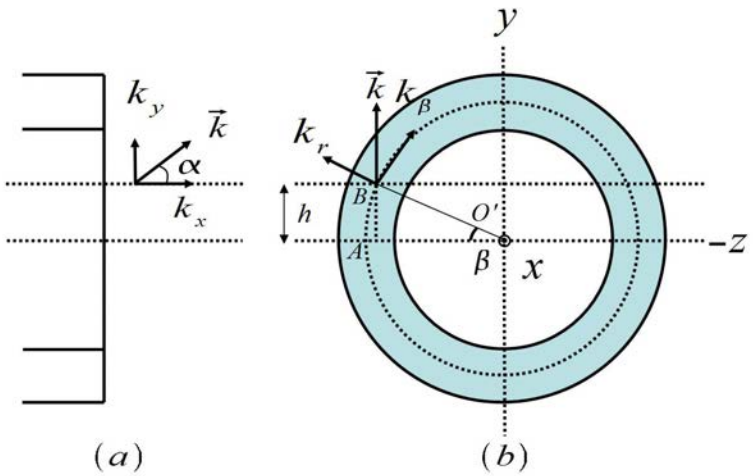

Figure 7. Positioning of measurement volume at different heights h with respect to thruster axis results in different values of k_r. (a) shows a side view of the thruster and k_x and k_y components; (b) shows the thruster face and k_r and k_β components.

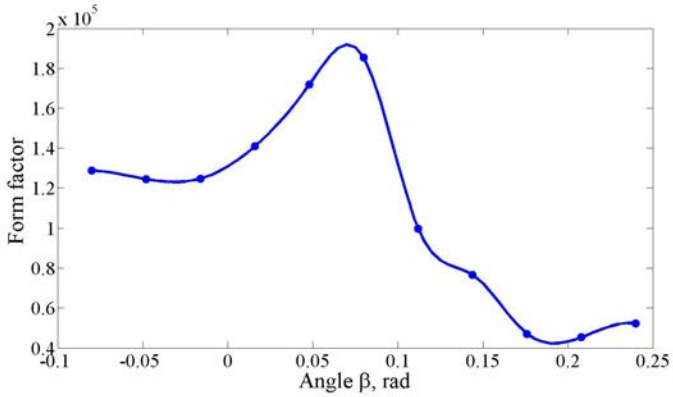

Figure 8. Variation of form factor with β

at a value of 5900 rad/m, and the form factor amplitude determined. The variation of the form factor with height is shown in Fig. 8, where h is related to β by

$$\sin\beta = h/R \tag{4}$$

It has been repeatedly observed that the maximum in amplitude for this mode is obtained not when measurements are on-axis, but rather when the measurement volume is 5 mm above the axis, i.e. for $\beta = 0.08$ rad.

E. The electron density fluctuation rate

With the newly-determined spatial distributions of the $\vec{E} \times \vec{B}$ mode, the density fluctuation rate may be calculated. The density fluctuation $\langle \tilde{n}^2 \rangle$ is related to the form factor by

$$\langle \tilde{n}^2 \rangle = \frac{n_0}{(2\pi)^3} \int S(\vec{k}) dk^3 \tag{5}$$

n_0 is the mean plasma density. From the results for the distribution of the mode in the planes (k_x, k_y) and (k_y, k_z), Eq. 5 becomes

$$\langle \tilde{n}^2 \rangle \approx \frac{S_0 n_0}{(2\pi)^3} \int_0^\infty dk\, e^{-kb} \int_0^{2\pi} d\alpha\, k e^{-\frac{(\alpha-\mu_\alpha)^2}{2\sigma_\alpha{}^2}} k\Delta\beta \tag{6}$$

Equation 6 contains the following elements: (i) the exponential dependence of $S(k)$ on k, with parameters S_0 and b determined from Eq. 3, (ii) the Gaussian form of $S(k)$ as a function of α, a distribution centered about $\mu_\alpha = 10.6°$ and of peak width $\sigma_\alpha = 3.6°$, and (iii) the width $\Delta\beta$, approximately 0.15 rad. The resulting integral form is

$$\langle \tilde{n}^2 \rangle \approx \frac{\sigma_\alpha \Delta\beta}{2^{3/2}\pi^{5/2} b^3} n_0 L \tag{7}$$

where L is the plasma scattering length, 50 mm (i.e. twice the thruster channel width).

Hence

$$\langle \tilde{n}^2 \rangle \approx 0.76 \times 10^{31} m^{-6} \tag{8}$$

The corresponding r.m.s density fluctuation is 2.76×10^{15} m^{-3}. The density fluctuation rate is determined by a normalization of this value by the mean electron density, which is taken to be 10^{18} m^{-3} (a reasonable value, but one which is not accurately known).

In this case, the r.m.s density fluctuation rate is

$$\frac{\sqrt{\langle \tilde{n}^2 \rangle}}{n_0} = 2.8 \times 10^{-3} \tag{9}$$

This value is very small, around 0.3%. However, if the mean plasma density were 10^{17} m^{-3}, the corresponding fluctuation rate would be 3%. The measured signal amplitude itself is not sensitive to n_0, and is proportional only to the fluctuating density $\tilde{n}^2$.

The degree to which the signal level output by the bench is representative of the density fluctuation has been rigorously tested in two ways. First, the heterodyning efficiency of the optical bench has been determined using a specially-designed experiment and was found to be close to 1, indicating that any losses due to the manner in which the wave fronts of the local oscillator and plasma-scattered radiation superpose is negligible. Second, the signal output by the bench has been calibrated, through the use of a piezoelectric element to generate an acoustic wave of known amplitude. The predicted acoustic wave amplitude and that measured by the bench were found to be within 20% of each other.

IV. Conclusions

The results of this experimental study demonstrate the value of the collective light scattering diagnostic in determining the properties of high frequency, small-scale oscillations in the thruster plume. Our results for the frequencies and length scales of this azimuthally-propagating mode are consistent with numerical and theoretical predictions. Aside from agreements with theory, our experiments have revealed new aspects concerning this mode, such as its restricted direction of propagation, and that fact that it is not strictly aligned with $\vec{E}\times\vec{B}$, but slightly inclined inwards (towards the thruster) and possesses a component parallel to $\vec{B}$. The density fluctuation level of the mode has been measured. It is interesting to consider the consequences of the structure of this mode on the thruster and electron transport mechanisms.

Acknowledgments

The authors thank colleagues A. Héron and J.-C. Adam for valuable discussions on experimental and numerical results, and S. Mazouffre for advice on thruster physics. This work was performed with support from the French National Research Agency under Contract No. ANR-06-BLAN-0171-04, and with support from the Joint Research Program GDR No. 2759 CNRS/CNES/SNECMA/Universités *Propulsion Spatiale à Plasma*.

References

[1]Adam, J.C, Héron, A., and Laval, G., "Study of stationary plasma thrusters using two-dimensional fully kinetic simulations," *Phys. Plasmas*, Vol. 11, No. 1, 2004, pp. 295-305.

[2]Truc, A., Quéméneur, A., Hennequin, P., Grésillon, D., Gervais, F., Laviron, C., Olivain, J., Saha, S. K., and Devynck, P., "ALTAIR: An infrared laser scattering diagnostic on the TORE SUPRA tokamak," *Rev. Sci. Instrum.*, Vol. 63, No. 7, 1992, pp. 3716-3724.

[3]Tsikata, S., Lemoine, N., Pisarev, V., and Grésillon, D., "Dispersion relations of electron density fluctuations in a Hall thruster plasma, observed by collective light scattering," *Phys. Plasmas*, Vol. 16, 2009, pp. 033506-033506(10).

[4]Holzhauer, E. and Massig, J. H., "An analysis of optical mixing in plasma scattering experiments," *Plasma Phys.*, Vol. 20, 1978, pp. 867-877.